# Study of sulfur dioxide crossover in proton exchange membrane fuel cells

Junxiang Zhai [a,b], Ming Hou [a,*], Huabing Zhang [a,b], Zhimin Zhou [a,b], Jie Fu [a,b], Zhigang Shao [a,**], Baolian Yi [a]

[a] Fuel Cell System and Engineering Laboratory, Dalian Institute of Chemical Physics, Chinese Academy of Science, Zhongshan Road, Dalian 116023, China
[b] Graduate School of the Chinese Academy of Sciences, Beijing 100039, China

## ARTICLE INFO

## ABSTRACT

As one of the most deleterious impurities to proton exchange membrane fuel cells (PEMFCs), sulfur dioxide ($SO_2$) in air can pass through the membrane from the cathode to the anode and poison the catalyst of the two electrodes. The phenomenon of $SO_2$ crossover is investigated electrochemically in this paper. The influences of $SO_2$ concentration, relative humidity, gas pressure and current density on $SO_2$ crossover are discussed. Experimental results reveal that the anode tends to be poisoned heavily with the increasing concentration of $SO_2$ in the cathode. The coverage of the anode catalyst by $SO_2$ permeating from the cathode enlarges with the decreasing relative humidity in the anode. The rate of $SO_2$ crossover from the anode to the cathode is promoted at high current density when $SO_2$ is directly introduced into the anode side instead of the cathode side, which can be ascribed to the electro-osmotic drag effect. Gas pressures show no obvious effects on $SO_2$ crossover. A co-permeation mechanism of $SO_2$ with water is deduced based on the overall analysis.

## 1. Introduction

Proton exchange membrane fuel cells (PEMFCs) are usually considered as one of the most promising alternative power sources for transportation and stationary applications due to their high energy efficiency, zero emission and rapid start-up. Ambient air, which always contains impurities ($NO_x$, $SO_x$, CO, etc.), is commonly used as the cathode oxidant in PEMFCs. Among those impurities, sulfur dioxide ($SO_2$) is almost the most deleterious to the performance of PEMFCs [1].

The effect of $SO_2$ on PEMFC performance has been widely studied. The cell performance decreased by 53% and by 78% after the cell exposure to 2.5 ppm and 5 ppm $SO_2$–air mixture, respectively [2]. Jing et al. [3] demonstrated that 35% decay on the cell performance was found when the cell was exposed to 1 ppm $SO_2$ for 100 h. Moreover, 0.25 ppm $SO_2$–air mixture could dramatically degrade the cell performance [4]. The pollution mechanism of $SO_2$ is also deeply investigated. Most researchers supported that $SO_2$ occupied the active sites of the catalyst by its adsorption on the platinum catalyst and thus decreased the catalytic activities [2–4]. The modes of $SO_2$ adsorption on the platinum catalyst were distinguished into linear adsorption and bridged adsorption [5]. Fu et al. [6] investigated the potential dependence of $SO_2$ poisoning and oxidation. They suggested that $SO_2$ molecules could be adsorbed on the Pt catalyst without charge transfer at 0.65 V, oxidized above 0.65 V and reduced below it. To date, some methods, such as cycle voltammogram (CV) scans, open circuit voltage (OCV) and *I–V* measurements, have already been used to handle with $SO_2$ poisoning [2,7,8]. Additionally, Ma et al. [9] confirmed that activated carbon could be used as air filtration adsorbent to prevent $SO_2$ from poisoning the cell catalyst.

Degradation of PEMFC performance caused by $SO_2$ in air is intrinsically due to $SO_2$ adsorption on the platinum surface of the cathode catalyst. Recently, several researchers have found that some impurities could migrate through the membrane from one side of the cell into the other side and poison the platinum catalyst on the two sides. Qi et al. [10,11] studied the effect of CO in the anode on the performance of the PEMFC cathode. They found that CO could migrate through the membrane to poison the cathode catalyst and cause dramatic performance degradation. It was also reported that $H_2S$ in hydrogen could pass through the electrolyte membrane, and damage the cathode catalyst [12]. Furthermore, Brosha et al. [13] measured the rates of $H_2S$ crossover with an ion-probe technique. Under their experimental conditions, the calculated rates of $H_2S$ crossover varied from $7.58 \times 10^{-10}$ to $4.65 \times 10^{-9}$ g s$^{-1}$ atm$^{-1}$ cm$^{-1}$. The phenomenon of $SO_2$ crossover in PEMFCs has also been reported in Refs. [14,15]. They found that $SO_2$ in the cathode could permeate through the membrane into the anode, and poison the catalyst of the two electrodes. Useful results

* Corresponding author. Tel.: +86 411 84379051; fax: +86 411 84379185.
** Co-corresponding author. Tel.: +86 411 84379153; fax: +86 411 84379185.
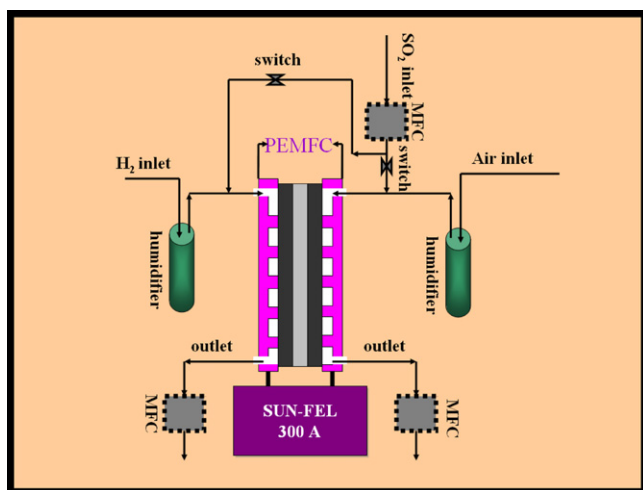*E-mail addresses:* houming@dicp.ac.cn (M. Hou), zhgshao@dicp.ac.cn (Z. Shao).

**Fig. 1.** Schematic diagram of the fuel cell system.



**Fig. 2.** Cyclic voltammograms obtained after the cathode exposure to 15 ppm $SO_2$–air for 2 h at 500 mA cm$^{-2}$. Operating pressure: $P_{air}$ = 0.1 MPa; humidification temperatures of the anode and cathode: 70 °C and 70 °C. (a) CV curves of the cathode; (b) CV curves of the anode, the insert is the enlarged part of CV curves of hydrogen peaks.

have been given in the references mentioned above. However, the mechanism and the influence factors of $SO_2$ crossover still need to be further explored.

In this paper, we implemented detailed studies on the phenomenon of $SO_2$ crossover. CV measurements were performed on both the cathode and the anode to detect behaviors of $SO_2$ poisoning. The mechanism of $SO_2$ crossover was also discussed.

## 2. Experimental

In this study, all experiments were carried out in a single cell with an active area of 5 cm$^2$. A Nafion® 212 membrane (Dupont) was sandwiched by two commercial gas diffusion electrodes (Sunrise Power Co., Ltd.) and hot-pressed to form a membrane-electrode-assembly (MEA). The Pt loadings for both of the cathodic and anodic electrodes were 0.4 mg cm$^{-2}$. The parallel flow field was machined on the flexible graphite, and the cell was then tightened using stainless steel endplates, seal rubber, bolts and nuts.

The cell temperature was constantly kept at 70 °C during all experiments. The flow rates of $H_2$ and air were 50 and 1000 sccm (standard cubic centimeters per minute), respectively. The operating pressure of the anode side was 0.1 MPa. Other parameters, such as relative humidification (RH), the operating pressure of the cathode side ($P_{air}$) and $SO_2$ concentration, were adjusted according to the experimental arrangement. Flows of $H_2$ and air were separately controlled by a mass flow controller (Beijing Sevenstar Electronics Co., Ltd.) fixed at the electrode outlet. The flux of $SO_2$ was controlled by the mass flow controller at the electrode inlet. $SO_2$ was mixed with the humidified air or $H_2$ in order to avoid $SO_2$ dissolving in water and adsorbing in the humidifier. The schematic diagram of the fuel cell system is shown in Fig. 1.

The single cell was tested with a constant-current mode by SUN-FEL 300 A (Sunrise Power Co., Ltd.). The voltage–time ($V$–$t$) curves could be automatically recorded in a computer. Thus, the decay of the voltage could be observed during the continuous injection of $SO_2$. After the cell was exposed to $SO_2$ for a certain time, the cyclic voltammetry (CV) measurements were performed by using a PARSTAT 2273 electrochemical station (America, EG&G Instruments Corp.). The applied potential range was from 0.05 to 1.4 V versus dynamic hydrogen electrode (DHE), and the scan rate was 50 mV s$^{-1}$. During CV experiments, when the cathode (or the anode) was acting as the working electrode with $N_2$ purging, the anode (or the cathode) was correspondingly acting as the reference and counter electrodes with pure $H_2$ supply.
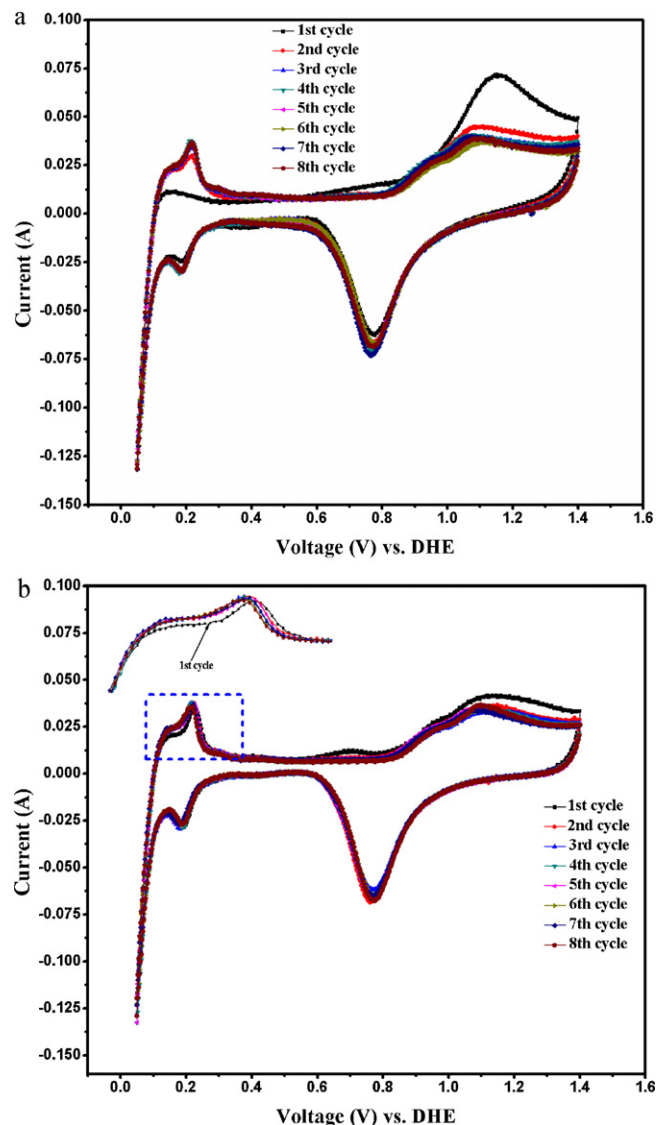
## 3. Results and discussion

### 3.1. The phenomenon of $SO_2$ crossover in PEMFCs

Fig. 2 shows the variations of eight CV cycles for both of the cathode and the anode after the cathode side was exposed to 15 ppm $SO_2$–air mixture at 500 mA cm$^{-2}$ for 2 h. The anode was fed with pure hydrogen. During the experiment, the relative humidities in the anode and cathode sides were all kept at 100%, and the pressures of reacting gases in the cathode and the anode were both 0.1 MPa. Fig. 2(a) shows the typical CV curves after $SO_2$ poisoning the cathode catalyst. It can be seen that the current peak on the first cycle differs from the followings. The current peak of hydrogen-desorption is lower, while that of oxygen oxidation is higher than the corresponding current peaks on the following scans. According to the report in Ref. [6], the reduced hydrogen-desorption peak is attributed to $SO_2$ adsorption and occupation on active sites of the cathode catalyst. The large oxidation peak is formed when the potential reaches about 1.1 V, at which $SO_2$ adsorption on

platinum catalyst is electro-oxidized. The corresponding electrochemical reactions are shown in the following equations:

$$2Pt–SO_2 + O_2 \rightarrow 2Pt–SO_3 \tag{1}$$

$$Pt–SO_3 + H_2O \rightarrow Pt + H_2SO_4 \tag{2}$$
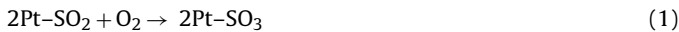
In the subsequent CV cycles, the oxidation peaks of $SO_2$ disappear and the peaks of hydrogen-desorption reemerge and finally overlap. This also means that all adsorbed $SO_2$ on the catalyst is removed. According to Refs. [16,17], when adsorbed sulfur species are removed from the platinum catalyst, the voltammogram for the final several CVs of the poisoned catalyst is almost identical to the CV of the fresh catalyst. The final CVs of the poisoned electrode and the CV of the fresh electrode may not fully overlap because of the complex of cells, but they are very colse, which could be both observed in Refs. [18,19]. Therefore, the final CV of the poisoned electrode is regarded as the CV of the fresh electrode in the whole text.

Due to the high sensitivity of the platinum catalyst, CV measurements were chosen to detect if there was any $SO_2$ on the platinum catalyst of the anode. In this operation, the anode was acting as the working electrode with $N_2$ purging and the cathode as the reference and counting electrodes with pure $H_2$ supply. Results are shown in Fig. 2(b). From Fig. 2(b), it can be seen that the hydrogen-desorption peak on the first cycle is slightly smaller than that on the subsequent cycles. The inset of Fig. 2(b) clearly shows that there is the distinct difference between the peak areas of hydrogen-desorption on the first cycle and that on the following cycles. Moreover, an additional oxidation peak is observed at about 1.1 V for the anode during the first positive scan. In the following cycles, the additional oxidation peaks disappear, and the hydrogen-desorption peaks almost overlap. These results indicate that the active sites of the anode catalyst are occupied by some impurity.

By comparing Fig. 2(b) with Fig. 2(a), it indicates that characters of CV curves of the anode are similar to that of the cathode. The hydrogen-desorption peaks on the first cycle at both of the anode and the cathode are smaller than that on the following cycles. An additional peak caused by the oxidation of some impurity appears at a potential of about 1.1 V on the first cycle, and disappears in the subsequent cycles. Then the corresponding peaks almost overlap with each other. Because $SO_2$ in the cathode is the only impurity during the whole experiment, it can be concluded that the impurity adsorbed on the anode catalyst could be $SO_2$, which migrates from the cathode side to the anode side.

Fig. 3 shows the variations of eight cyclic voltammetry curves of the anode after the cathode exposure to 1 ppm $SO_2$–air mixture at a current density of 500 mA cm$^{-2}$ for 10 h. The results are similar to that of the cathode exposure to 15 ppm $SO_2$–air mixture. It can be seen that the hydrogen-desorption peak on the first cycle is smaller than that on the subsequent cycles, and an additional oxidation peak appears at a potential of about 1.1 V. With the increase in the CV cycles, the oxidation peaks become smaller and the hydrogen-desorption peaks become larger. It indicates that even if the concentration of $SO_2$ in air is extremely low, $SO_2$ can still pass through the electrolyte membrane to the anode and poison the anode catalyst.

### 3.2. SO₂ crossover in PEMFCs under various conditions

#### 3.2.1. Effect of the relative humidity (RH) difference between the anode and the cathode on SO₂ crossover

The pressures of the cathode and the anode sides were both kept at 0.1 MPa. 15 ppm $SO_2$–air mixture was supplied into the cathode at 500 mA cm$^{-2}$. The humidity levels in the cathode and the anode (expressed as $c$RH and $a$RH) were 100% and 14%, respectively. After the cell was poisoned by $SO_2$ for 2 h, eight CV cycles were car-
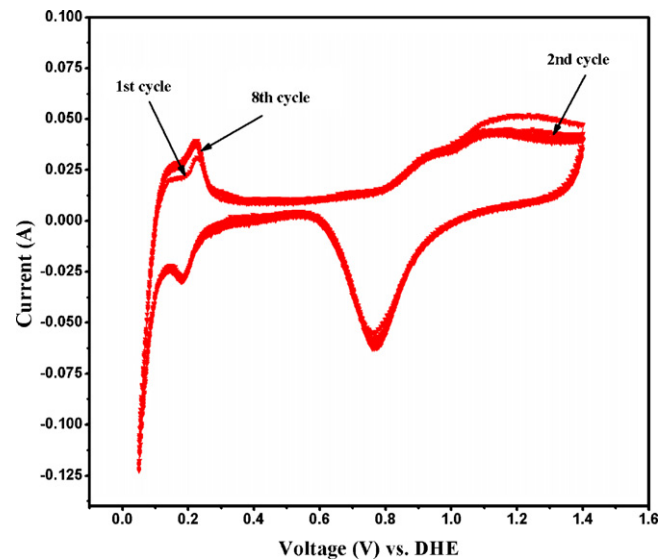


**Fig. 3.** Cyclic voltammograms of the anode obtained after the cathode exposure to 1 ppm $SO_2$–air for 10 h at 500 mA cm$^{-2}$. Operating pressure: $P_{air}$ = 0.1 MPa; humidification temperatures of the anode and cathode: 70 °C and 70 °C.

ried out for the anode. CV curves on the first and the eighth cycles are shown in Fig. 4(a). From Fig. 4(a), it can be observed that the hydrogen-desorption peak on the first cycle is smaller than that on the eighth cycle, which means that $SO_2$ migrates through the membrane into the anode side and occupies the Pt active sites. The oxidation peak on the first cycle is bigger than that on the eighth cycle at the potential of about 1.1 V, which indicates that the impurity is electro-oxidized at this potential. Finally, the hydrogen-desorption peaks recover and the $SO_2$ oxidation peaks diminish gradually in the sequential CV cycles. Fig. 4(b) shows the CV curves of the anode side when $a$RH and $c$RH were both 100%. Similar results are obtained. The ratio of the hydrogen-desorption peak area on the first cycle to that on the eighth cycle is expressed as Eq. (3):

$$\theta_H = \frac{\theta_{1st}}{\theta_{8th}} \tag{3}$$

In this equation, $\theta_{1st}$ is the hydrogen-desorption peak area on the first cycle, $\theta_{8th}$ is the hydrogen-desorption peak area on the eighth cycle. Therefore, $\theta_H$ may denote the active sites of the platinum catalyst for hydrogen desorption after the cell is poisoned. Correspondingly, $SO_2$ coverage of the catalyst can be expressed as Eq. (4):

$$\theta_{poisoning} = 1 - \theta_H \tag{4}$$

Here, $\theta_{poisoning}$ denotes the coverage of $SO_2$ on the platinum catalyst. In the case of $a$RH = $c$RH = 100%, $\theta_H$ is equal to 98%, which indicates that the $\theta_{poisoning}$ is 2%. In the case of $a$RH (14%) < $c$RH (100%), $\theta_H$ is equal to 76%, which indicates that $\theta_{poisoning}$ is 24%. Therefore, the anode catalyst is more severely poisoned in the latter case. Under the condition of $a$RH < $c$RH, the relative humidity in the anode is lower than that in the cathode, so water transport is promoted from the cathode to the anode across the electrolyte membrane due to back diffusion. The water transport also assists $SO_2$ migrating from the cathode to the anode, which leads to a more severe contamination in the anode catalyst.

Fig. 5 shows the comparison of CV curves on the first cycle after the cell was poisoned by $SO_2$ under different humidification conditions. From Fig. 5, it can be seen clearly that more platinum active sites of the anode catalyst are occupied by $SO_2$ when the relative humidity in the anode is lower than that in the cathode. The crossover rate of $SO_2$ is proportional to the difference of the relative humidity between the cathode and the anode.
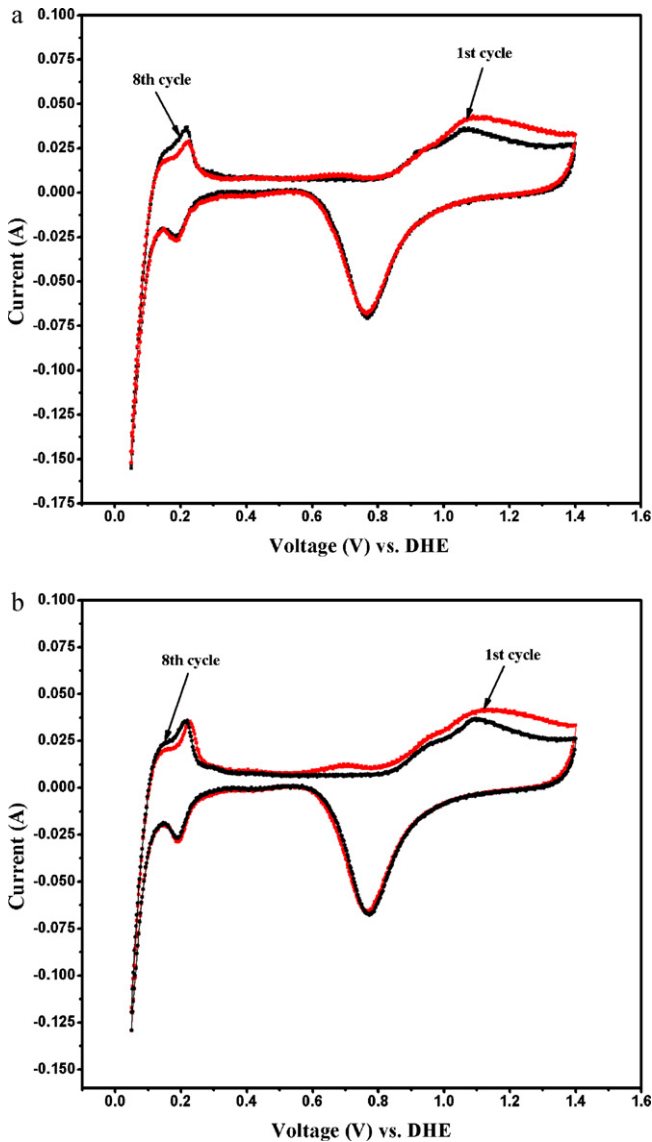
a



b

**Fig. 4.** Cyclic voltammograms of the anode obtained after the cathode exposure to 15 ppm $SO_2$–air for 2 h at 500 mA cm$^{-2}$. Operating pressure: $P_{air} = 0.1$ MPa; $c$RH: constant at 100% (a) humidification temperatures of the anode and the cathode: 40 °C and 70 °C; $a$RH 14%; (b) humidification temperatures of the anode and the cathode: 70 °C and 70 °C; $a$RH 100%.

As it is well known, $SO_2$ can easily dissolve in water with a volume ratio of 40:1. Thus, the majority of $SO_2$ dissolves in water. A portion of $SO_2$ dissolved in water adsorbs on the catalyst surface, and the rest transports to the other side accompanying with water. As a result, the dissolution of $SO_2$ plays a role in assisting $SO_2$ migration.

### 3.2.2. Effect of gas pressures on $SO_2$ crossover

The relative humidities in both the anode and the cathode were kept at 100%. The anode pressure was kept at 0.1 MPa, while the cathode pressure was adjusted to 0.1 MPa, 0.14 MPa and 0.18 MPa. 15 ppm $SO_2$–air mixture was fed into the cathode at a current density of 500 mA cm$^{-2}$ for 2 h. Fig. 6 shows the comparison of CV curves of the anode at different cathode pressures. It can be seen that CV curves on the first cycle almost overlap with each other under the three cathode pressures above-mentioned. It indicates that gas pressures have no obvious effect on $SO_2$ crossover. The reason could be that the difference of gas pressures between the anode
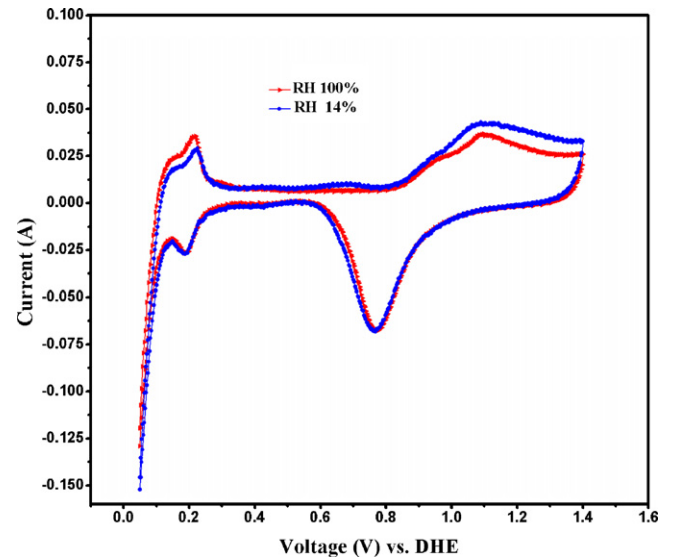


**Fig. 5.** Comparison of CV curves of the anode on the first cycle. $a$RH: varied from 14% to 100%; $c$RH: constant at 100%.

and the cathode had little influence on water transport, which was previously reported by Chai et al. [20].

### 3.2.3. Effect of $SO_2$ concentrations on $SO_2$ crossover

The cathode pressure was kept at 0.1 MPa. $c$RH and $a$RH were all 100%. $SO_2$ in air with different concentrations was fed into the cathode at a current density of 500 mA cm$^{-2}$ for 2 h. CV scans were performed on the anode after the cell was poisoned. $\theta_H$ and $\theta_{poisoning}$ were calculated and summarized in Table 1. From Table 1, it can be seen that $\theta_H$ is 98%, 87% and 80% under the $SO_2$ concentrations of 15 ppm, 20 ppm and 30 ppm, respectively. Thus, the coverage of the anode catalyst, $\theta_{poisoning}$, is 2%, 13% and 20%, respectively. The higher the $SO_2$ concentration is, the higher the coverage of $SO_2$ is. The anode catalyst is more and more severely deteriorated with the increase in $SO_2$ concentrations, which points out that more $SO_2$ permeates across the membrane from the cathode into the anode. $SO_2$ crossover rate is proportional to the concentration
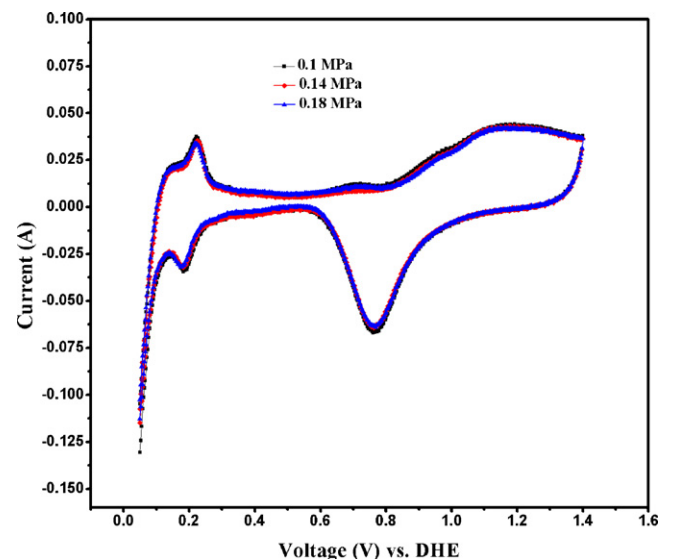


**Fig. 6.** Comparison of CV curves of the anode on the first cycle obtained after the cathode exposure to different gas pressures with 15 ppm $SO_2$–air for 2 h at 500 mA cm$^{-2}$. Humidification temperature of the anode and cathode: 70 °C and 70 °C; operating pressure: $P_{H_2} = 0.1$ MPa, $P_{air} = 0.1$–0.18 MPa.

**Table 1**
Effect of SO$_2$ with different concentrations on SO$_2$ crossover.

| | Concentration (ppm) | | |
| --- | --- | --- | --- |
| | 15 | 20 | 30 |
| $\theta_H$ (%) | 98 | 87 | 80 |
| $\theta_{poisoning}$ (%) | 2 | 13 | 20 |

gradient. The concentration should be related to the concentration of SO$_2$ in water due to the dissolution of SO$_2$.

### 3.2.4. Effect of the electro-osmotic drag on SO$_2$ crossover

Another factor, which influences the water transport, is the electro-osmotic drag (water molecules are dragged by protons migrating from the anode to the cathode). Based on this point, a special experiment was carried out by directly supplying SO$_2$ into the anode side. 15 ppm SO$_2$–H$_2$ mixture was fed into the anode at different current densities for 2 h. The relative humidities in the anode and the cathode were all 100%. The pressures in the anode and the cathode were both kept at 0.1 MPa. CV scans were performed on the cathode after the cell was poisoned.

Fig. 7 shows the CV curves of the cathode obtained after the cell ran at 500 mA cm$^{-2}$. The insert is the enlarged section of the hydrogen-desorption peaks on the first cycle and the eighth cycle. From the insert, it is clearly observed that the hydrogen-desorption peak on the first cycle is smaller than that on the eighth cycle. It indicates that a part of active sites of the cathode catalyst are occupied by some impurity. When the scan potential gets more positive, a tiny additional current appears at about 1.1 V, which is caused by the electro-oxidization of the impurity. As it is known, SO$_2$ in H$_2$ is the only impurity in the whole experiment. Therefore, the impurity adsorbed on the cathode catalyst can be only the impurity of SO$_2$ which migrates from the anode. Under this condition, $\theta_H$ is 90%, which indicates that 10% active sites of the cathode catalyst are covered by SO$_2$ migrating from the anode. Fig. 8 shows the CV curves of the cathode obtained after the cell ran at 1000 mA cm$^{-2}$. Under this condition, $\theta_H$ is about 78%. Correspondingly, the coverage of SO$_2$ is about 22%. Obviously, the cathode catalyst is more severely
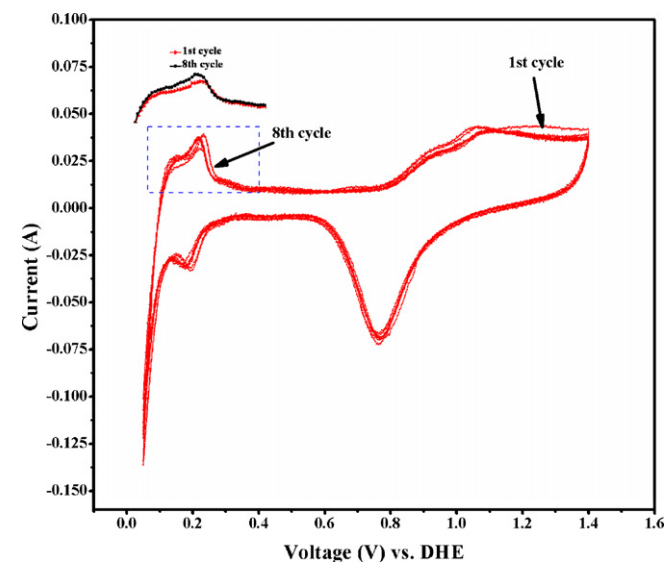


**Fig. 8.** Cyclic voltammograms of the cathode obtained after the anode exposure to 15 ppm SO$_2$–H$_2$ for 2 h when the cell ran at current density of 1000 mA cm$^{-2}$. Operating pressure: $P_{air} = P_{H_2} = 0.1$ MPa; humidification temperatures of the anode and the cathode: 70 °C and 70 °C.

contaminated by SO$_2$ from the anode under the condition of higher current density. As it is known, more water transports from the anode to the cathode due to the electro-osmotic drag when the cell is operated at a higher current density. Therefore, more SO$_2$ dissolves in water and permeates into the cathode from the anode.

From all the experiments above, it can be concluded that SO$_2$ mainly transports through the membrane via water. It means that the mechanism of SO$_2$ crossover might be a co-permeation mechanism of SO$_2$ with water. The sketch of the supposed mechanism is described in Fig. 9. SO$_2$ arrives at the catalyst layer of MEA through the gas diffusion layer. A portion of that adsorbs on the catalyst surface, and the rest migrates across the electrolyte membrane together with water into the other side of MEA.

In the present study, we mainly paid attention to the behaviors of SO$_2$ crossover and tried to explore the mechanism of SO$_2$ crossover. The accurate rate of SO$_2$ crossover and how SO$_2$ crossover affects the anode overpotential will be the focus of our future work.



**Fig. 7.** Cyclic voltammograms of the cathode obtained after the anode exposure to 15 ppm SO$_2$–H$_2$ with for 2 h when the cell ran at 500 mA cm$^{-2}$. Operating pressure: $P_{air} = P_{H_2} = 0.1$ MPa; humidification temperatures of the anode and cathode: 70 °C and 70 °C. The insert is the enlarged part of CV curves of hydrogen peaks on the first cycle and on the eighth.
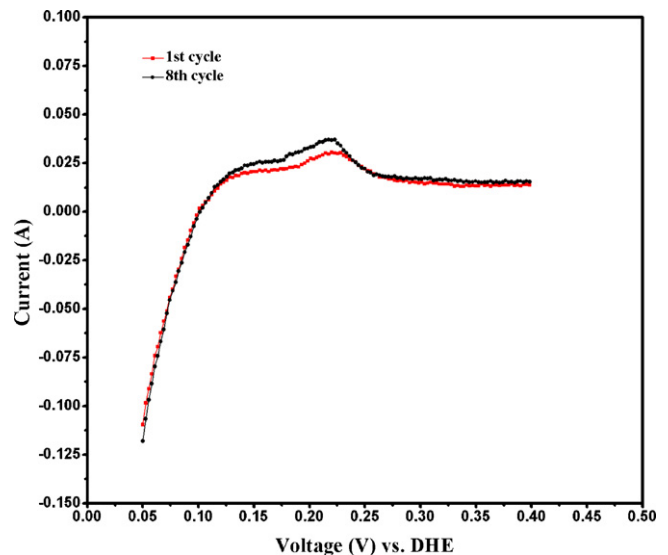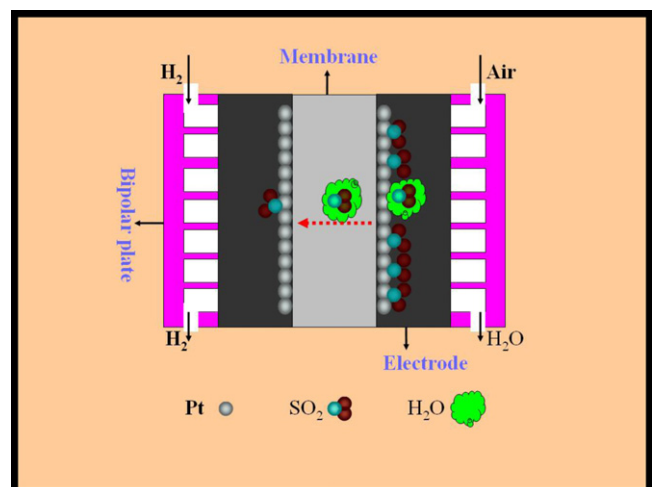


**Fig. 9.** Sketch of the mechanism of SO$_2$ crossover: co-permeation with water.

## 4. Conclusions

The phenomenon of $SO_2$ crossover in PEMFCs was studied. $SO_2$ in air could migrate across the membrane from the cathode to the anode, adsorb on the anode catalyst and occupy the active sites. The phenomenon of $SO_2$ crossover even occurred in the presence of trace amount of about 1 ppm. $SO_2$ crossover depended on various conditions including relative humidity, concentration gradient and current density, while gas pressures had no obvious effect on it. When the relative humidity in the anode was lower than that in the cathode, more active sites of the anode catalyst would be covered by $SO_2$ from the cathode. The coverage of the anode catalyst was 2%, 13% and 20% under the $SO_2$ concentrations of 15 ppm, 20 ppm and 30 ppm, respectively. It indicated that the anode catalyst was more seriously contaminated with an increase in $SO_2$ concentration in the cathode side. When $SO_2$ was directly fed into the anode, $SO_2$ crossover rate was higher at 1000 mA cm$^{-2}$ than that at 500 mA cm$^{-2}$. This was because more water molecules passed through the membrane into the cathode by the electro-osmotic drag, and it led to a more serious $SO_2$ crossover by $SO_2$ dissolution in water. Thus, it was concluded that the $SO_2$ crossover mechanism could be the co-permeation of $SO_2$ with water.

## Acknowledgement

## References

[1] S. Knights, N. Jia, C. Clug, J. Zhang, Fuel Cell Seminar, 2005.
[2] R. Mohtadi, W. Lee, J.W. Van Zee, J. Power Sources 138 (2004) 216–225.
[3] F. Jing, M. Hou, W. Shi, J. Fu, H. Yu, P. Ming, J. Power Sources 166 (2007) 172–176.
[4] E. Brosha, F. Garzon, B. Pivovar, T. Rockward, J. Valeria, F. Uribe, 2005 Mid. Year DOE Fuel Cell Program Review, 2005.
[5] A.Q. Contractor, H. Lal, J. Electroanal. Chem. 103 (1979) 103–117.
[6] J. Fu, M. Hou, C. Du, Z. Shao, B. Yi, J. Power Sources 187 (2009) 32–38.
[7] F. Uribe, W. Smith, M. Wilson, FY 2003 Progress Report, LANL, 2003.
[8] B.D. Gould, O.A. Baturina, K.E. Swider-Lyons, J. Power Sources 188 (2009) 89–95.
[9] X. Ma, D. Yang, W. Zhou, C. Zhang, X. Pan, L. Xu, M. Wu, J. Ma, J. Power Sources 178 (2008) 383–389.
[10] Z. Qi, C. He, A. Kaufman, Electrochem. Solid-State Lett. 4 (12) (2001) A204–A205.
[11] Z. Qi, C. He, A. Kaufman, J. Power Sources 111 (2002) 239–247.
[12] F. Garzon, DOE Hydrogen Program, Los Alamos National Lab, 2007, pp. 1–20.
[13] E.L. Brosha, T. Rockward, F.A. Uribe, F.H. Garzon, J. Electrochem. Soc. 157 (2010) B180–B186.
[14] S. Tsushima, H. Morioka, K. Kaneko, S. Hirai, ECS Trans. 16 (2008) 1043–1050.
[15] Y. Zhai, G. Bender, S. Dorn, R. Rocheleau, J. Electrochem. Soc. 157 (2010) B20–B26.
[16] Y. Garsany, O. Baturina, K. Swider-Lyons, J. Electrochem. Soc. 154 (7) (2007) B670–B675.
[17] Y. Garsany, O. Baturina, K. Swider-Lyons, J. Electrochem. Soc. 156 (7) (2009) B848–B855.
[18] D. Imamura, Y. Hashimasa, ECS Trans. 11 (1) (2007) 853–862.
[19] F. Garzon, 2009 DOE Hydrogen Program Annual Review: Effects of Fuel and Air Impurities on PEM Fuel Cell Performance. Los Alamos National Lab, 2009.
[20] Y. Chai, J. Hu, B. Yi, H. Zhang, Chin. J. Power Sources 29 (2005) 659–662.